

WOJCIECH BURLIKOWSKI, ZYGMUNT KOWALIK*

ERROR ANALYSIS IN MATHEMATICAL MODEL OF ELECTROMECHANICAL ACTUATOR USING HAMILTONIAN EQUATIONS

ANALIZA BŁĘDU W MODELU MATEMATYCZNYM PRZETWORNIKA ELEKTROMECHANICZNEGO WYKORZYSTUJĄCYM RÓWNANIA HAMILTONA

Abstract

This paper presents a methodology of error analysis in a mathematical model of an electromechanical actuator using Hamiltonian equations in the description of energy conversion. As the basic quantity in numerical algorithms, the coenergy of magnetic field E_{cm} is employed. The reason for the application of coenergy as a state function is the explicitness of its value for a given set of state variables, resulting from neglecting eddy currents and hysteresis phenomenon in the model.

Keywords: electrical machines, Hamiltonian equations, error analysis, relative error

Streszczenie

W artykule przedstawiono metodykę analizy błędów w modelu matematycznym przetwornika elektromechanicznego wykorzystującym równania Hamiltona w opisie przemiany elektromechanicznej. Jako podstawowej wielkości w algorytmie obliczeniowym użyto koenergii pola magnetycznego E_{cm} . Wykorzystano w tym celu jednoznaczność określenia wartości koenergii dla danej wartości zmiennych stanu, wynikającą z pominięcia w modelu prądów wirowych oraz zjawiska histerezy.

Słowa kluczowe: maszyny elektryczne, równania Hamiltona, analiza błędów, błąd względny

DOI: 10.4467/2353737XCT.15.033.3833

* D.Sc. Ph.D. Eng. Wojciech Burlikowski, M.Sc. Eng. Zygmunt Kowalik, Department of Mechatronics, Faculty of Electrical Engineering, Silesian University of Technology, Gliwice.

1. Introduction

In the case of electromechanical actuators, the main advantage of the Hamiltonian model compared to equivalent Lagrangian model is the canonical form of its equations [11]. This feature is particularly important in the computer implementation of this model due to the possible application of discrete databases concerning only currents and flux linkages as the input values. These values can be obtained using numerical analysis (e.g. using the finite elements method FEM [3, 4]) or through measurements. Due to the lack of a method for determining magnetic field coenergy by measurements, it is assumed that it is not available during the mathematical model construction, although there are numerical methods for its determination [8].

2. Error sources

Independently of the method for determining the input values, in the simulation model there are possible errors, the sources of which are:

- a) simplicial approximation – this is a topological method of current-flux characteristic approximation based on the triangulation of the discrete databases which define this characteristic,
- b) uncertainty of currents and flux values related to numerical (using FEM, [8]) or measurement [10] errors.

In this paper, an error resulting from the first source mentioned above is analysed. As the measure of this error, a local deviation ΔE_{cm} from explicitness of the coenergy computation inside a single simplex from a triangulated current set is taken [1, 3, 6]. The obtained results are compared with a mathematically equivalent reciprocity principle, relating to the symmetry of the dynamic inductance matrix in the case of an electromechanical actuator [11]. The mechanical equation was not considered as the analysis concerns a constant rotor angular position $\vartheta = \text{const}$ (Fig. 1).

3. Canonical equations

In the paper, a 3-phase synchronous reluctance machine SynRM with wye-connected stator windings without neutral wire is analysed as an exemplary electromechanical actuator (Fig. 1) [2]. The differential equation describing an electrical part of the model is:

$$\mathbf{e} = \frac{d\Psi}{dt} + \mathbf{R}\mathbf{i} \quad (1)$$

where:

$$\mathbf{i} = [i_A, i_B]^T$$

– the generalized currents vector,

$$\Psi = [\Psi_{AC}, \Psi_{BC}]^T = [\Psi_A - \Psi_C, \Psi_B - \Psi_C]^T$$

– the generalized flux linkages vector,

$$\mathbf{e} = [e_{AC}, e_{BC}]^T$$

– the generalized external voltages vector,

\mathbf{R}

– resistance matrix.

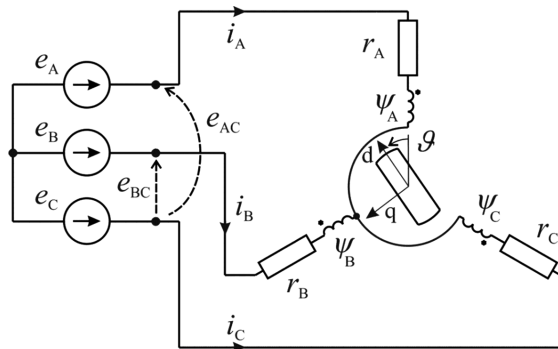


Fig. 1. A scheme of a SynRM machine

The choice of considering the wye-connected stator windings without neutral wire is made because of its great practical importance, as well as it ensuring the lowest possible state space dimension $N = 2$, which allows the electromechanical system as a whole to be graphically analysed [4].

Obtaining a set of canonical equations based on equation (1) requires setting state variables and dependent variables. The choice leads to one of the two forms of canonical equations [4, 11]:

- a) Hamilton equations, in which flux linkages are state variables (such a model is called HMEA – Hamiltonian Model of Electromechanical Actuator):

$$\frac{d\Psi}{dt} = \mathbf{e} - \mathbf{R}\mathbf{i}(\vartheta, \Psi) \quad (2)$$

- b) Lagrange equations, in which **currents** are state variables:

$$\frac{d\mathbf{i}}{dt} = (\mathbf{L}_d(\vartheta, \mathbf{i}))^{-1} \left(\mathbf{e} - \left(\omega \frac{\partial \Psi(\vartheta, \mathbf{i})}{\partial \vartheta} + \mathbf{R}\mathbf{i} \right) \right) \quad (3)$$

where:

ω – mechanical angular velocity of the rotor,

$\mathbf{L}_d(\vartheta, \mathbf{i})$ – dynamic inductance matrix [11].

4. Synergy features used in HMEA

In the considered electromechanical system, there are no elements that store potential energy. In this case, coenergy E_{cm} can be expressed as a scalar product of two generalized quantities relating to the magnetic field:

$$E_{cm}(\vartheta, \mathbf{i}) = \int_0^{\mathbf{i}} \Psi \cdot d\mathbf{i} \quad (4)$$

Due to the fact that coenergy is a state function of the considered system, its change along a closed path equals zero:

$$\oint \Psi \cdot d\mathbf{i} = 0 \quad (5)$$

It allows a flux linkage vector field defined in the current space \mathbf{RI} (which is, for $N = 2$, a subspace of a three-dimensional Euclidean space E^3 with a standard basis $[\vec{e}_{iA} \ \vec{e}_{iB} \ \vec{e}_{iC}]$) to be interpreted as a curlless field (Stokes' theorem):

$$\text{rot } \Psi = \begin{vmatrix} \vec{e}_{iA} & \vec{e}_{iB} & \vec{e}_{iC} \\ \frac{\partial}{\partial i_A} & \frac{\partial}{\partial i_B} & 0 \\ \Psi_{AC} & \Psi_{BC} & 0 \end{vmatrix} = \mathbf{0} \quad (6)$$

which yields:

$$\vec{e}_{iC} \left(\frac{\partial \Psi_{AC}}{\partial i_B} - \frac{\partial \Psi_{BC}}{\partial i_A} \right) = \mathbf{0} \quad (7)$$

and is equivalent to the symmetry of the dynamic inductance matrix $\mathbf{L}_d(\vartheta, \mathbf{i})$ of the analysed system.

5. Discrete model of the electromechanical actuator

The discrete model is formulated using data collected by a numerical analysis using the FEM method and a FEMM computer program [7]. A FEM model of a prototype SynRM machine was created. This prototype machine is based on a stator from a mass produced RSg 80-4A induction motor by the BESEL company. Its basic characteristic features, fundamental for a mathematical model construction, are as follows:

- Rated current $I_n = 2.2 \text{ A}$,
- Number of stator poles $2p = 4$,
- Number of stator slots $Q_s = 36$,
- Number of rotor poles $Q_r = 4$,
- Rotor's length $l_r = 72 \text{ mm}$,
- Number of turns per slot $z_s = 90$,
- Air gap length $\delta = 0.25 \text{ mm}$.

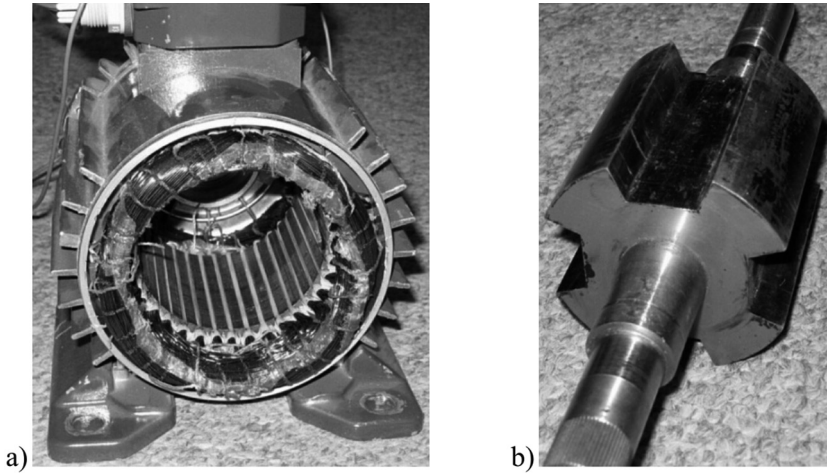


Fig. 2. A pictorial view of a stator (a) and a rotor (b) of a modeled SynRM machine

The numerical analysis was made for a currents set I^k , which is a Cartesian product of a sequence $I = \{-4 \text{ A}; -3.5 \text{ A}; \dots; 4 \text{ A}\}$, i.e. $I^k = I \times I$. For each point $\mathbf{i}_p \in I^k$ (Fig. 3) a flux linkages vector Ψ_p was computed, thus constructing a set $\Psi^k = \{\Psi_1, \Psi_1, \dots, \Psi_K\}$, K – number of points (Fig. 4). The set Ψ^k is a subset of a flux linkage space $\mathbf{R}\Psi \subset E^N$.

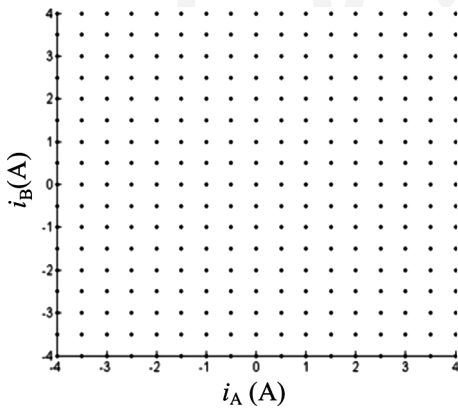


Fig. 3. Currents set I^k

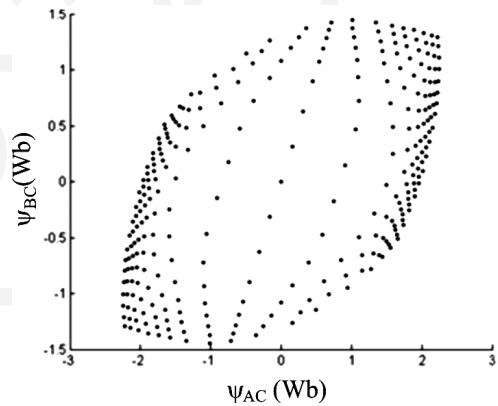


Fig. 4. Flux linkages set Ψ^k

6. Error definition in HMEA

Due to a homeomorphism between currents space \mathbf{RI} and flux linkages space $\mathbf{R}\Psi$, coming from assumed uniqueness of magnetization characteristic, further analysis concerns a T^k triangulation defined on a set I^k using Delaunay algorithm (Fig. 5) [1, 6]. The triangulation result is a simplex grid (which are triangles for $N = 2$), which enables flux linkage computation in every point of space \mathbf{RI} using the simplicial approximation [3, 6].

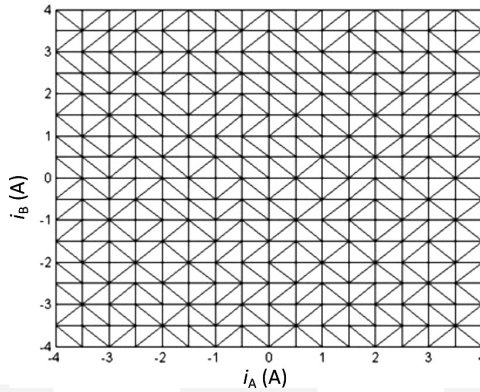


Fig. 5. Currents subspace triangulation $T^k(I^k)$

Because flux linkage values, obtained either from numerical analysis or measurements, are taken with an error and because of the use of simplicial approximation, coenergy in every simplex is computed with an error. Therefore, the influence of this error value generated by both of the aforementioned factors on the computed integral values needs to be explored [9]. As a measure of this error, a local deviation ΔE_{cm} from explicitness of the coenergy computation inside each simplex $\Delta_{I,j}^k$ of the triangulated currents set is used:

$$\oint_{\partial S_I} \Psi \cdot d\mathbf{i} = \Delta E_{cm} \tag{8}$$

where:

∂S_I – analysed simplex boundary (Fig. 6).

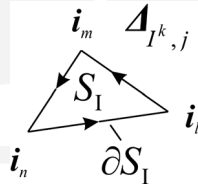


Fig. 6. A Simplex S_I in the currents subspace

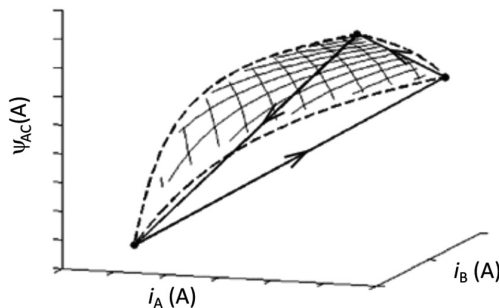


Fig. 7. Graphical interpretation of the error related to the curvature of the current-flux characteristic

The ΔE_{cm} value is equal to 0 for an accurate values of currents and flux linkages (dashed line, Fig. 7). For a linear approximation of a current-flux characteristic an error appears (solid line, Fig. 7).

The exact measure of an error for a given simplex $\Delta_{l,j}^k$ is a relative error value expressed as [10]:

$$\delta E_{cm} = \frac{\Delta E_{cm}}{\bar{E}_{cm}} \quad (9)$$

where \bar{E}_{cm} – average value of coenergy in a given simplex (Fig. 6).

For simplicity, \bar{E}_{cm} is defined as an arithmetical average of the coenergy value in the vertices of a given simplex [4].

7. Error definition in a Lagrangian model

Similar to the HMEA, a relative error in a model based on Lagrange equations was defined. As a measure of it, a violation rate of the reciprocity principle was chosen. This error is related to the symmetry of the dynamic inductance matrix:

$$\Delta L_d = \frac{\partial \Psi_{AC}}{\partial i_B} - \frac{\partial \Psi_{BC}}{\partial i_A} \quad (10)$$

According to equations (5) and (7), this value is an analogue to the ΔE_{cm} parameter expressed by equation (8). The relative error value is defined as:

$$\delta L_d = 2 \frac{\Delta L_d}{\left(\left| \frac{\partial \Psi_{AC}}{\partial i_B} \right| + \left| \frac{\partial \Psi_{BC}}{\partial i_A} \right| \right)} \quad (11)$$

In formulas (10) and (11) for the derivatives approximation a central difference algorithm is used [9].

8. Computational results

In Figures 8–10, it can be seen that in both cases, the absolute error value is the largest at the transition between the linear area of the current-flux characteristic and the area in which magnetic saturation is observed (Fig. 10).

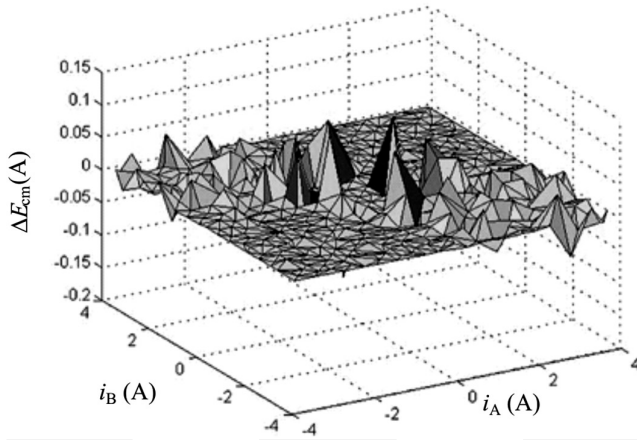


Fig. 8. Absolute error in HMEA

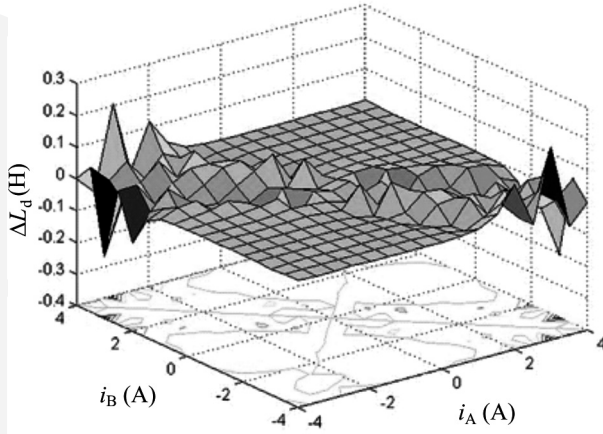


Fig. 9. Absolute error in the Lagrangian model

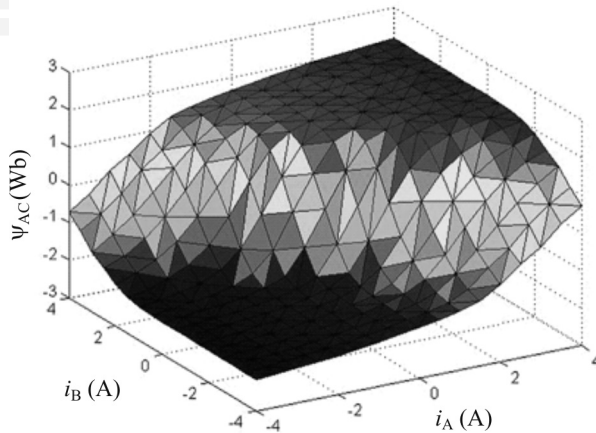


Fig. 10. Current flux characteristic $\psi_{AC}(i_A, i_B, \vartheta = 30^\circ)$

This result is as expected as in this region, the curvature of the current-flux characteristic is the highest (Fig. 10). These results are consistent with the computed relative error values in the HMEA model (Fig. 11). In the case of the Lagrangian model, a relative error distribution is far from prediction (Fig. 12).

For computation, a rotor angular position $\vartheta = 30^\circ$ is chosen, as a coupling between generalized windings is the largest for this angular position [3, 4].

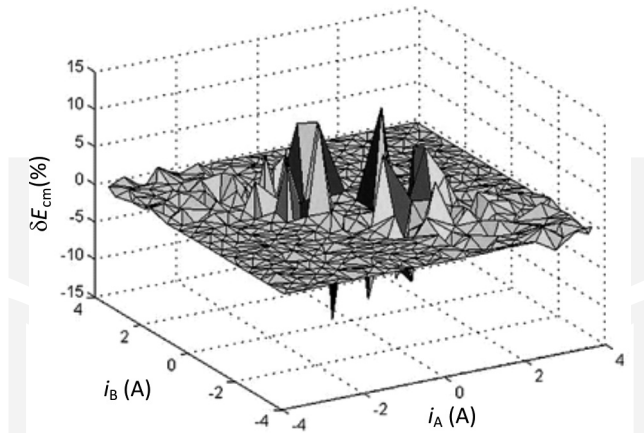


Fig. 11. Relative error in HMEA

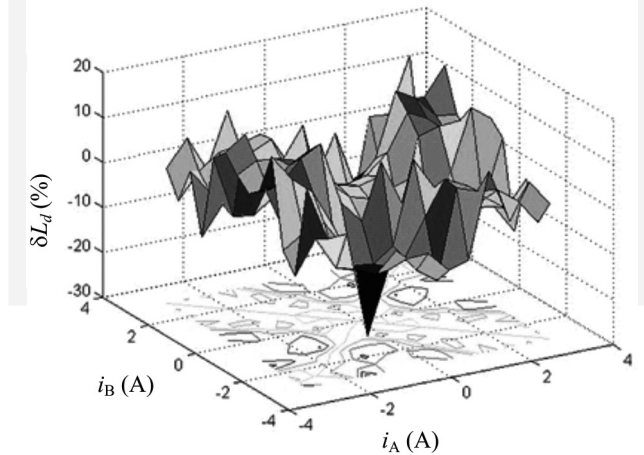


Fig. 12. Relative error in Lagrange model

9. Conclusions

General conclusions that come from the comparison between relative errors in both the HMEA and Lagrangian model are as follows:

- a) relative error range is similar in both cases (15%–20%),
- b) a possible simple algorithm of error minimization can be used in HMEA (barycentric subdivision [6]) due to the lack of necessity of complicated numerical differentiation [9]. This results in a reduction of the region, where computed errors are the largest, to the region of the highest curvature of the current-flux characteristic (Fig. 10),
- c) there is a necessity for much more precise methods for computing elements of dynamic inductance matrix in the Lagrangian model. It has to be done probably as early as during FEM numerical analysis [5],
- d) in case of the Lagrangian model, a relative error distribution is stochastic in the whole analysed currents subspace (Fig. 12), which makes its minimization harder, as it requires increased database accuracy in the whole considered range.

References

- [1] Agoston M.K., *Computer Graphics and Geometric Modeling – Mathematics*, Springer, 2005.
- [2] Boldea I., Tutelea L., *Electric machines: steady state, transients and design with Matlab*, CRC Press, 2009.
- [3] Burlikowski W., *Reluctance motor mathematical model in natural reference frame using hamiltonian equations – simulational analysis*, Zeszyty Problemowe – Maszyny Elektryczne, 2011, nr 93, BOBRME Komel, pp. 19–24.
- [4] Burlikowski W., *Zastosowanie formalizmu Hamiltona w opisie przetwornika elektromechanicznego na przykładzie silnika reluktancyjnego*, Zeszyty Naukowe Politechniki Śląskiej „Elektryka”, Monografia, z. 373, Gliwice 2012.
- [5] Demenko A., Hameyer K., *Field and field-circuit description of electrical machines*, Proc. of EPE-PEMC 2008, pp. 2412–2419.
- [6] Kuratowski K., *Wstęp do teorii mnogości i topologii*, PWN, Warszawa 2004.
- [7] Meeker D., *Finite Element Method Magnetics. User's Manual*, ver. 4.2, 2007.
- [8] Meunier G. et al., *The Finite Element Method for Electromagnetic Modeling*, ISTE Ltd, 2008.
- [9] Ralston A., *Wstęp do analizy numerycznej*, wyd. 3, PWN, Warszawa 1983.
- [10] Skubis T., *Opracowanie wyników pomiarów: przykłady*, Wydawnictwo Politechniki Śląskiej, Gliwice 2003.
- [11] Sobczyk T.J., *Metodyczne aspekty modelowania maszyn elektrycznych prądu przemiennego*, WNT, Warszawa 2004.